GOCE OBSERVATIONS FOR DETECTING UNKNOWN TECTONIC FEATURES

Braitenberg C.[(1)], Mariani P.[(1)], Reguzzoni M.[(2)], Ussami N.[(3)]

(1) *Department of Geosciences, University of Trieste, via Weiss 1, 34100, Trieste, Italy, email: berg@units.it*
(2) *Geophysics of the Lithosphere Department - OGS, c/o Politecnico di Milano - Polo Regionale di Como, Via Valleggio 11, 22100 Como, Italy*
(3) *Departamento de Geofisica, Instituto de Astronomia, Geofísica e Ciências Atmosféricas, Universidade de São Paulo, Rua do Matão 1226, 05508-090, São Paulo, Brazil*

ABSTRACT

The global coverage of a satellite allows us to investigate areas that are difficult to access due to remoteness or ruggedness. We intend to use the GOCE gradiometric observations to detect unknown tectonic features. At the present stage of the GOCE mission we take the error levels of the observations to estimate the resolution of known density discontinuities of the Earth crust: the crust-mantle and sediment-basement transition. The spherical harmonic expansion of mass distributions is compared with the estimated degree error curves of the gravity field. We find that the GOCE data will contribute to a better resolution of these discontinuities by one order of magnitude for degree between 52 and 200 compared to the EGM2008 gravity field model. The geodynamic context affects the resolution as it controls the average Moho depth, shallower levels being better resolved. For the basement the dominant resolution parameter is the density contrast across the interface.

1. INTRODUCTION

The GOCE satellite is the first mission to carry a gravity gradiometer on board with the goal of improving knowledge of the global Earth gravitational field. It was launched on 17th March 2009 and has been acquiring data since then, following a 6-month calibration phase. The goal of our work is to estimate the geologically relevant structures which can be usefully studied with the GOCE data. We intend to estimate the spatial frequency range in which the GOCE satellite data can be used to improve existing global gravity models.

We consider the crust-mantle interface (Moho) and the top basement, both giving rise to important density variations which are near-ubiquitous in the Earth crust. We consider continental areas because in oceanic areas the field derived from satellite altimetry (e.g. [1]) has a superior spatial resolution. The existing global gravity models (e.g. [2],[3]) are defined by their development in spherical harmonics of the gravitational potential V:

$$V(r,\varphi,\lambda) = \frac{GM}{r} \left(1 + \sum_{n=1}^{N}\sum_{k=0}^{n}\left(\frac{R_e}{r}\right)^n \left(C_{nk}\cos k\lambda + S_{nk}\sin k\lambda\right)\overline{P}_{nk}(\sin\varphi)\right) \quad (1)$$

The field is defined by the Stokes coefficients C_{nk} and S_{nk} and their relative errors, δC_{nk}, δS_{nk}. N is the maximum degree of the expansion, G the gravitational constant, M the Earth mass, r the geocentric distance, φ the latitude, λ the longitude of the computation point, R_e the equatorial radius of the Earth ellipsoid. The degree error C_n is defined as:

$$C_n = \sqrt{\sum_{k=0}^{n}\left(\delta C_{nk}^2 + \delta S_{nk}^2\right)} \quad (2)$$

Since the field and its error are expressed in spherical harmonics, it is natural to carry out the sensitivity analysis in the harmonic expansion of the mass. We consider a spherical shell of radius R, thickness $t(\varphi,\lambda)$ and volume density $\rho(\varphi,\lambda)$. We may define the surface density as $m(\varphi,\lambda) = t(\varphi,\lambda)\cdot\rho(\varphi,\lambda)$. The surface density is expanded in terms of spherical harmonics leading to:

$$m(\varphi,\lambda) = \sum_n m_n(\varphi,\lambda)$$
$$m_n(\varphi,\lambda) = \sum_{n,k}\left(a_{nk}\cos k\lambda + b_{nk}\sin k\lambda\right)\overline{P}_{nk}(\sin\varphi) \quad (3)$$

The disturbing potential T generated by such a mass distribution is given by:

$$T(r,\varphi,\lambda) = \sum_n T_n = \sum_n \frac{4\pi GR}{2n+1}\left(\frac{R}{r}\right)^{n+1} m_n \quad (4)$$

The gravity anomaly Δg is:

Proc. 'ESA Living Planet Symposium', Bergen, Norway
28 June – 2 July 2010 (ESA SP-686, December 2010)

$$\Delta g(r,\varphi,\lambda) = \sum_n \Delta g_n = \sum_n \frac{4\pi G}{2n+1}(n-1)\left(\frac{R}{r}\right)^{n+2} m_n \qquad (5)$$

The vertical gravity gradient component T_{zz} is:

$$T_{zz}(r,\varphi,\lambda) = \sum_n T_{zz\,n} = \sum_n \frac{4\pi G}{2n+1}\frac{(n+1)(n+2)}{R}\left(\frac{R}{r}\right)^{n+3} m_n \qquad (6)$$

The half-wavelength of a feature on the Earth surface corresponding to the harmonic expansion complete up to degree and order n is [4]:

$$s = \frac{2\sqrt{\pi}R_e}{n+1} = \frac{22600}{n+1}[km] \qquad (7)$$

The GOCE satellite is expected to contribute to the gravity field up to degree and order 200, which corresponds to a half-wavelength of 112 km.
The relations (4)-(6) can be used either to compute the fields for a given mass or, vice versa, to compute the mass from a given field. We use these relations to determine the smallest surface density that can be detected, given the degree error of the field. We consider the mass to be either at the level of the crust-mantle boundary, or at the level of the basement. We compare the error curve of the recent harmonic development of [3] with that expected for the GOCE mission.

2. DEGREE ERROR CURVES

The error-values of the Stokes coefficients for the EGM2008 model are published together with the Stokes coefficients. We convert the degree error-values to an error in terms of gravity anomalies as follows:

$$\delta\Delta g_n(r) = \frac{GM}{R_e^2}(n-1)\left(\frac{R_e}{r}\right)^{n+2} C_n \qquad (8)$$

with GM=3986004.415 10^8 m^3s^{-2} and R_e=6378136.3 m.

For comparison we use the error degree median values for GOCE. The calculations are based on the simulated data of the End to End simulation [5] for the AR3 test of the High Level Processing Facility [6]. The spherical harmonic coefficients were derived with the so-called space-wise approach [7] by combining the gravitational potential estimated from kinematic orbits with the simulated gravity gradients observed by the on-board gradiometer. The absolute error is significantly degraded

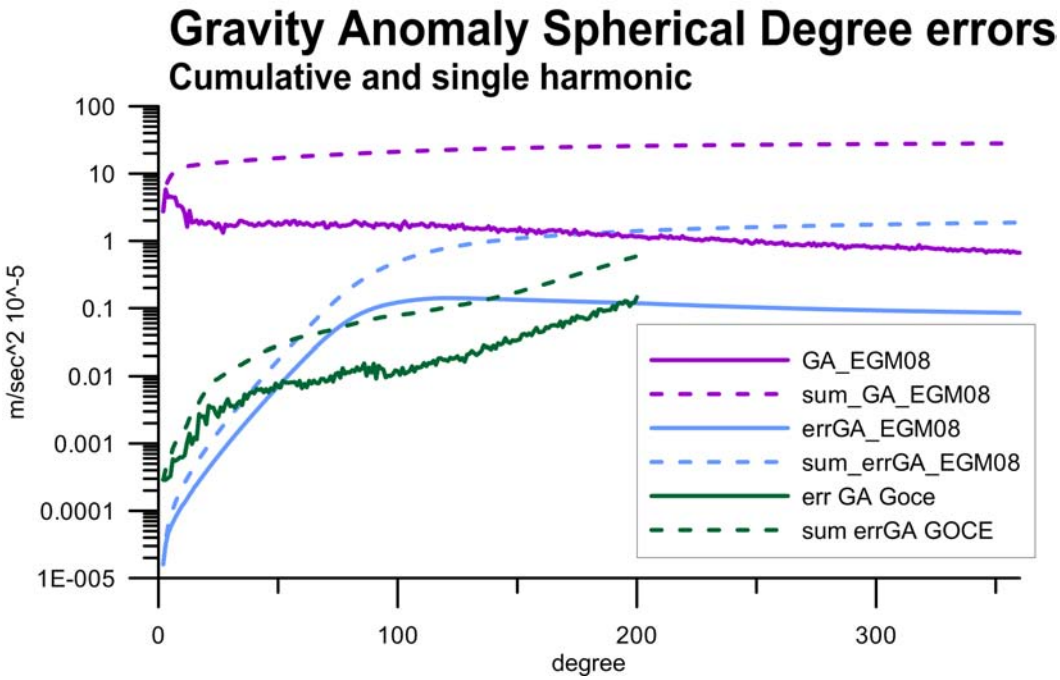

Figure 1: Single degree error of gravity anomaly (errGA) derived from the error degree variances of the gravity model EGM2008 and from the simulated GOCE error degree median. The cumulative error curves (sum_errGA) are also shown. GA_EGM08 is the degree amplitude of the gravity anomaly and sumGA_EGM08 the cumulative degree amplitude (model EGM08)

at low orders due to the polar gaps (GOCE orbital inclination of 96.7°), which is the reason why the degree error is estimated by degree medians and not by degree variances. The latter would be too much influenced by the effects of the polar gaps and would overestimate the error. In Fig. 1 the error curves for both models are shown, converted to errors of gravity anomaly. For degrees up to 120 the EGM2008 model mostly contains satellite gravity observations, for higher degrees the field stems from terrestrial data. The uncertainty for the simulated GOCE gravity anomalies is smaller than the existing gravity model EGM2008 for degrees between 52 and 200. The window changes slightly when considering the cumulative error curves, with smaller errors for GOCE between degree 58 and 200.

3. RESOLUTION OF THE CRUST-MANTLE INTERFACE AND OF THE BASEMENT

The resolution of the Moho is estimated considering a spherical shell at average depth d with surface density:

$$m(\varphi,\lambda) = \rho(\varphi,\lambda)\cdot t(\varphi,\lambda) \tag{9}$$

with thickness t and density ρ. The surface density can be interpreted as the oscillation of the crust-mantle boundary about the average depth d. In that case we may assume a constant density equal to $\delta\rho$, the density difference between crust and mantle; δt is then the amplitude of the oscillation. An analogous approach was used with a flat sheet mass in [8,9]. Given the degree error $\delta\Delta g_n$ of the gravity anomaly, the resolution of the expansion terms of the surface density is derived from equation (5) and (8) and yields:

$$\begin{aligned}\delta m_n &= \frac{2n+1}{4\pi G(n-1)}\left(\frac{r}{R_e-d}\right)^{n+2}\delta\Delta g_n(r)\\ &= \frac{(2n+1)M}{4\pi R_e^2}\left(\frac{R_e}{R_e-d}\right)^{n+2}C_n\end{aligned} \tag{10}$$

In terms of oscillation amplitude the resolution at degree n is:

$$\delta t_n = \frac{(2n+1)M}{4\pi R_e^2}\left(\frac{R_e}{R_e-d}\right)^{n+2}\frac{1}{\delta\rho}C_n \tag{11}$$

The Moho resolution at degree n depends on the degree error and on the average depth of the interface. In turn, the average depth depends on the geodynamic context. The nuclei of continental plates are formed by cratons, the oldest crustal components, with Moho depths near 45 km. Extreme Moho depths are found below high topographic plateaus (e.g. Tibetan plateau), with average depths of 70 km over large areas up to 500 km in extent. The Moho resolution degrades with increasing depth (equation 11).

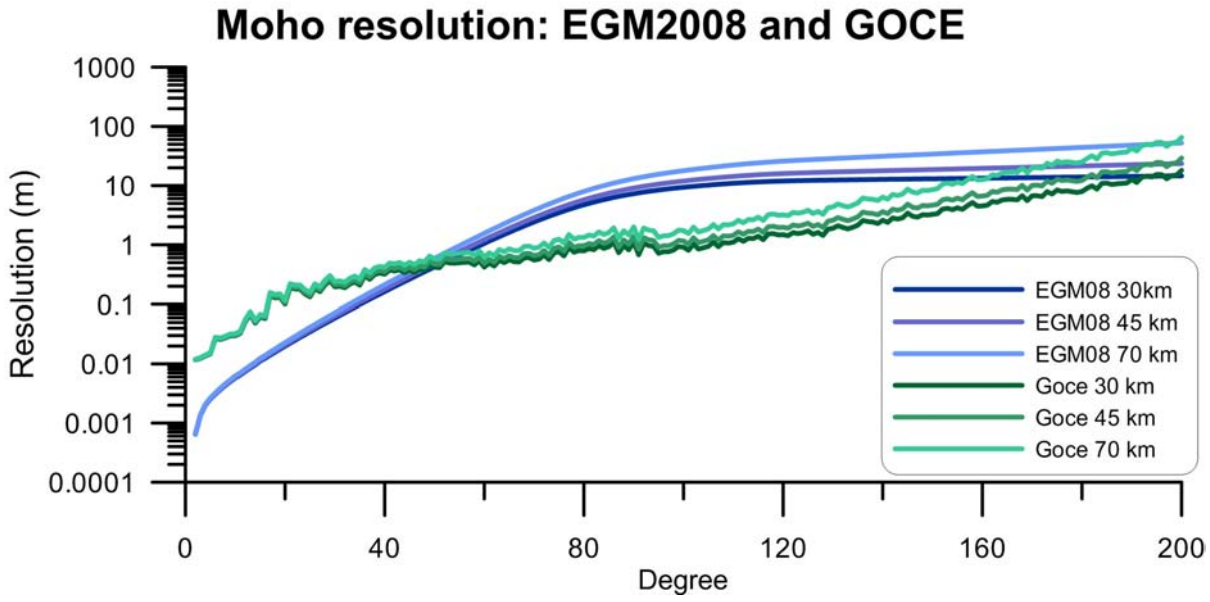

Figure 2: Resolution of Moho undulations. Average depth between 30 km and 70 km. Density across interface: 500 kg/m^3. Based on single degree error curve of global gravity model EGM2008 and the simulated GOCE error degree median

In Fig. 2 the errors based on the simulated GOCE and the EGM2008 single degree error curves are shown. We have set the density contrast equal to 500 kg/m^3 and the average depth equal to 30 km, 45 km and 70 km. We find an improvement by using the GOCE gravity model for degrees 52 to 200. The average depth affects resolution decisively, reducing it by almost an order of magnitude at degree 100 when passing from 30 km to 70 km. An example of a useful application is the Tibetan plateau where the spectral analysis [10;11] of the Bouguer field showed the presence of strong signals at wavelengths between 250 km and 400 km, well within the improved range.

The sediment-basement transition is an intracrustal boundary of common interest. Where a well defined density contrast between the two layers exists, this boundary can be treated with the same technique we used for the crust-mantle boundary. In this case the average depth is 0 to 10 km, the greater value corresponding roughly to half the thickness of deepest basins [12]. Realistic values for the density difference can be assumed to be 2700–2000 kg/m^3 = 700 kg/m^3 down to 2700–2650 kg/m^3 = 50 kg/m^3. We present a series of resolution curves that vary according to the density and reference depth. Inspecting equation (11) we deduce that resolution is inversely proportional to the density contrast and moderately dependent on the average thickness of the basins, d being much smaller than R_e. The curves are shown in Fig. 3: the variation due to d is hardly seen in the figure, the density variation being the dominant parameter. The basins we can investigate must be of large dimensions, with the short dimension greater than 112 km (half-wavelength of harmonic degree 200 using relation (7)). The cratonic and intracratonic basins are particularly suited as they are mostly of large dimensions: examples are the Tarim, Amazon, Michigan, North-Africa basins, Barents Sea, and West Siberian basin (e.g. [13]). These types of basins are not well understood, as they are set on thick crust and seem to be associated with anomalous upper mantle densities (example Barents Sea basins; [14]).

Another question concerns the sensitivity of the tensor components observed at GOCE satellite height compared to terrestrial measurements. Terrestrial gravity measurements are much more readily available than terrestrial tensor observations. This leads us to invert for the smallest crustal mass changes observable considering the error level of the potential second radial derivatives observed at the satellite height and that of the gravity anomalies obtainable with an airborne gravity campaign. Here we analyze both in terms of the information that can be retrieved for the crustal densities.
The degree error of the airborne gravity measurements is generally unavailable, so we have to estimate it starting from the average error level of an observation campaign. Referring to a root mean square (r.m.s.) measurement error $\delta\Delta g$, the degree error is here obtained

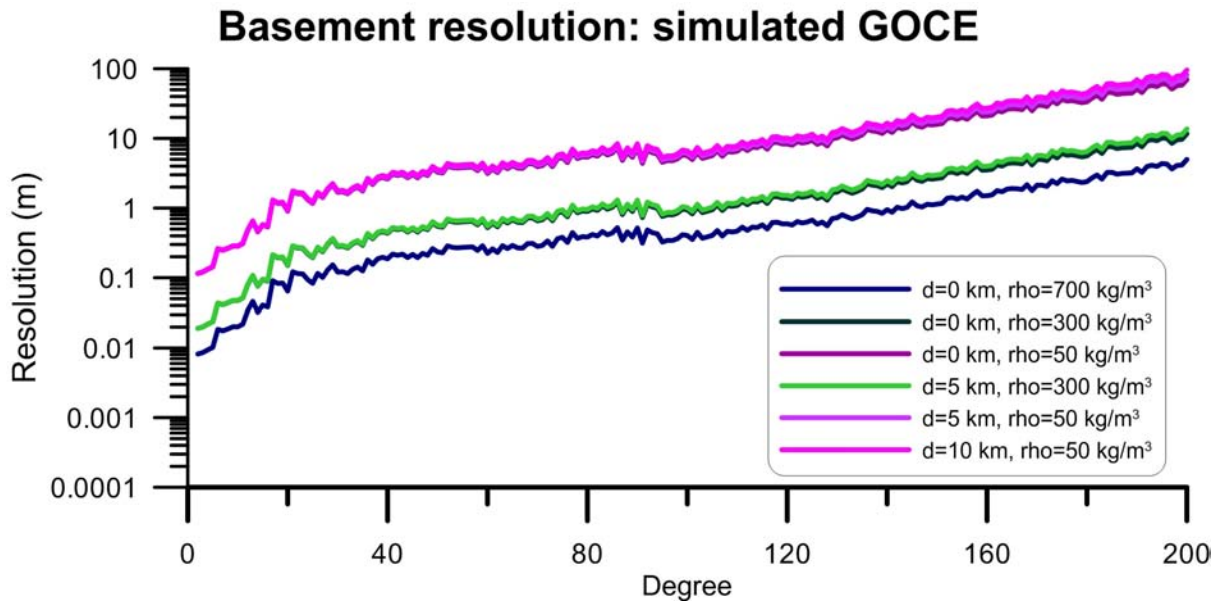

Figure 3: Resolution of top basement. Average depth between 0 km and 10 km. Density across interface: 700 to 50 kg/m^3. Based on simulated GOCE error degree median

assuming uniform distribution on each spherical harmonic component inside the degree interval defined by N_{min}=120 and N_{max}=200. The degree error $\delta\Delta g_n$ is then estimated by:

$$\delta\Delta g_n = \delta\Delta g \frac{\sqrt{(2n+1)}}{\sqrt{(N_{\max}+1)^2 - N_{\min}^2}} \tag{12}$$

With the aim of comparing gravity gradient and gravity anomaly error levels, we define the degree error of the potential second radial derivatives analogously, starting from the observation error r.m.s. δT_{zz} at satellite height. The estimated degree error is:

$$\delta T_{zz\,n} = \delta T_{zz} \frac{\sqrt{(2n+1)}}{\sqrt{(N_{\max}+1)^2 - N_{\min}^2}} \tag{13}$$

The density resolution of the spherical shell model assuming a fixed thickness k of the shell is given by resolving equation (9) for density:

$$\delta\rho(\varphi,\lambda) = \frac{\delta m(\varphi,\lambda)}{k} \tag{14}$$

Defining h as the height of the observation point, the smallest detectable density variation starting from gravity anomalies is:

$$\delta\rho_n = \frac{2n+1}{4\pi G(n-1)}\left(\frac{R_e+h}{R_e-d}\right)^{n+2}\frac{1}{k}\delta\Delta g_n \tag{15}$$

Starting from the potential second radial derivatives, it is:

$$\delta\rho_n = \frac{(2n+1)(R_e-d)}{4\pi G(n+1)(n+2)}\left(\frac{R_e+h}{R_e-d}\right)^{n+3}\frac{1}{k}\delta T_{zz\,n} \tag{16}$$

A useful example is the problem of defining the crustal density variation given the crustal thickness after correcting the observations for crustal inhomogeneities and mantle density variations. A problem of this sort is realistic, as the upper crust is accessible with active seismics and geological inferences and the mantle density can be deduced from global seismic tomography models (an example is treated in [15] discussing the West Siberian basin). Referring to this example of the West Siberian basin, the density variations of a

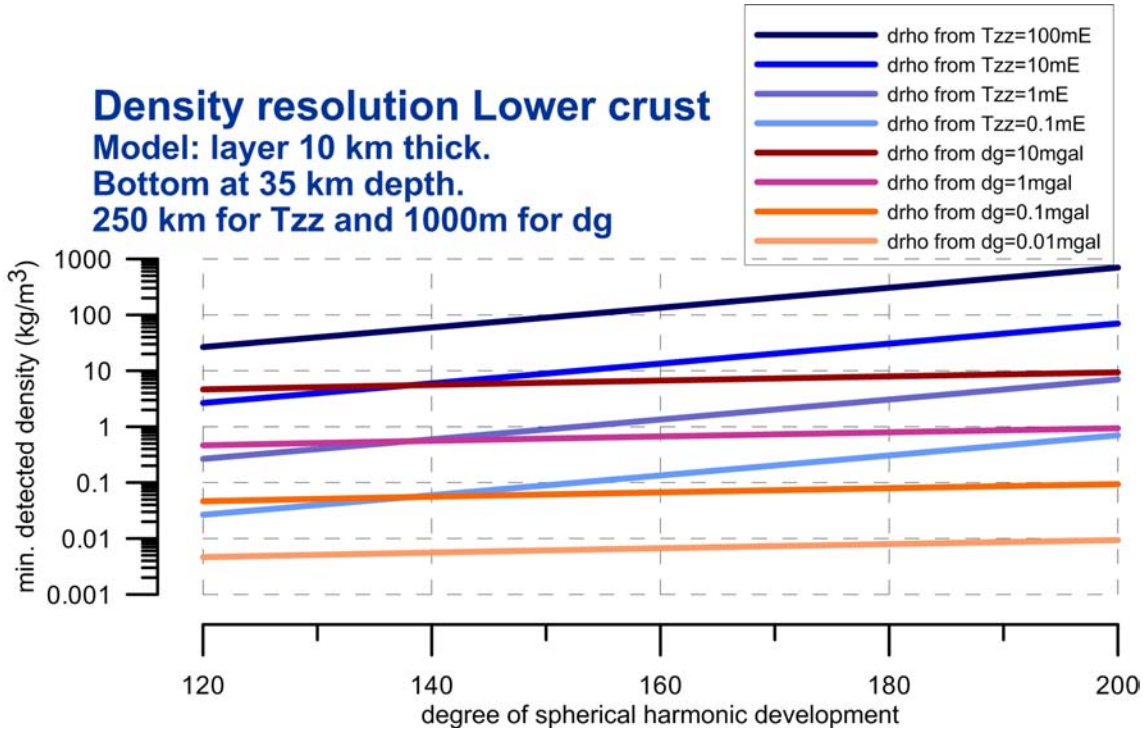

Figure 4: Resolution of density in the lower crust. Model: layer 10 km thick at the base of the crust, top at 30 km depth. Starting data: airborne gravity anomalies at 1000 m quota and satellite observed gravity gradients T_{zz} at 250 km quota. Different levels of measurement error

spherical shell with k=10 km thick, d=30 km depth, are inverted. In order to obtain a complete picture we make the error levels vary in a large range of values, covering 4 orders of magnitude, both for the gravity anomaly (equation 12) and for the vertical gravity gradient (equation 13). The error of T_{zz} observed at satellite height (250 km) is taken to be 0.1 mE, 1 mE, 10 mE and 100 mE. These values have been chosen considering the simulated r.m.s. error of T_{zz} along orbit, estimated to be 4 mE after various calibrations and filtering, and 550 mE before processing [7]; the error of Δg observed at 1000 m height is taken to be 0.01 mGal, 0.1 mGal, 1 mGal and 10 mGal. Typical noise in an airborne gravity survey is about 1 mGal at 4 km half-wavelength [16], but the error is greater at longer wavelengths. The smallest value (0.01 mGal) is probably unrealistic, but is used here as a reference. In Fig. 4 the level of density resolution of the lower crustal density layer is shown: starting from the airborne gravity data the degree has a very small effect, whereas for increasing degree the resolution worsens when using the T_{zz} at satellite height. At intermediate degree (n=140) the density resolution of the T_{zz} at satellite height with an r.m.s. of 10 mE is comparable to that of a gravity observation at 1000 m quota with a r.m.s. of 10 mGal.

4. DISCUSSION

Our goal is to use the GOCE data for improving knowledge of crustal structure. This can be done by using either the spherical harmonic development of the gravity field or directly the gradiometric measurements of GOCE at the satellite height. The model of a spherical shell inside Earth is convenient in our study because its expansion coefficients in spherical harmonics can be linked with a few scaling parameters directly to the gravitational potential and its functionals. In Cartesian coordinates a similar model is that of a plane sheet of varying density, or a boundary separating two layers of different density. Then the gravity field is calculated applying the well known Parker series expansion [17, 18] in the spectral domain. In the present work we used the degree errors of the gravity model to estimate the sensitivity in the density or the thickness of the shell. The values we found are the basis for the practical application that intends to find crustal density variations in a geologic area of interest. We have demonstrated that in a certain wavelength range GOCE will improve the resolution of the mass changes. In practice the observed field is due to mass changes in the entire crustal column, so the field contributions of different crustal depths must be separated before applying the inversion with the shell model. The recovery of crustal thickness variations or of density inhomogeneities at the base of the crust will depend very much on the ability to strip the observations from the superficial layers. In order to accomplish this task, the gravity data have to be integrated with models of the geologic context, knowledge of the geologic units and results on physical parameters as well as density obtainable from geophysical methods that retrieve seismic velocity, magnetic susceptibility or electrical conductivity.

5. CONCLUSION

The simulated degree error curve of the GOCE satellite was used to infer the smallest mass detectable either at the Moho or at upper crustal level. In the spherical harmonic expansion we find that for degrees between about 60 and 200 the improvement brought by GOCE should be about one order of magnitude in terms of detectable mass anomalies. This translates to an improvement in the detection of density anomalies or in the definition of crustal thickness variations. Concerning the basement depth variations at upper crustal levels, the resolution depends much more on the density contrast between sediments and basement than on the depth of the interface. The expected resolution of density changes in the lower crust using the observed tensor component T_{zz} at GOCE satellite height is comparable to that of an airborne gravity survey at 1000 m height with a root mean square error between 1 and 10 mGal at a spatial resolution of about 160 km. The relative performance of the satellite derived gravity gradient is better at longer wavelengths.

6. ACKNOWLEDGMENTS

This work contributes to the GOCE-Italy project of the Italian Space Agency and to the FAPESP project. The GOCE data are obtained under ESA AO ID 4323. We thank Alan Reid for revising the manuscript.

7. REFERENCES

1. Andersen O.B., Knudsen P., Berry P.A.M. (2010). *The DNSC08GRA global marine gravity field from double retracked satellite altimetry*, J. Geod., 84, 191-199, DOI: 10.1007/s00190-009-0355-9.
2. Förste C., Schmidt R., Stubenvoll R., Flechtner F., Meyer U., König R., Neumayer H., Biancale R., Lemoine J.-M., Bruinsma S., Loyer S., Barthelmes F., Esselhorn S. (2008). *The GeoForschungsZentrum Potsdam/Groupe de Recherche de Gèodésie Spatiale satellite-only and combined gravity field models: EIGEN-GL04S1 and EIGEN-GL04C*, J. Geod., 82, 331-346, DOI 10.1007/s00190-007-0183-8.
3. Pavlis N.K., Holmes S.A., Kenyon S.C., Factor J.K. (2008). *An Earth Gravitational Model to degree 2160: EGM2008*. Presented at the EGU General Assembly, Vienna, Austria, April 13-18, 2008.
4. Strang van Hees G.L. (2000). *Some elementary relations between mass distributions inside the Earth and the geoid and gravity field*, Journal of Geodynamics, 29, 111-123.

5. Catastini G., Cesare S., De Sanctis S., Dumontel M., Parisch M., Sechi G. (2007). *Predictions of the GOCE in-flight performances with the end-to-end system simulator*. Proc. of the 3rd International GOCE User Workshop, 6-8 November 2006, Frascati, Italy, (ESA SP-627, January 2007), 9-16.
6. Rummel R., Gruber T., Koop R. (2004). *High Level Processing Facility for GOCE: Products and Processing Strategy.* Proc. of the 2nd International GOCE User Workshop, 8-10 March 2004, Frascati, Italy, (ESA SP-569, June 2004).
7. Migliaccio F., Reguzzoni M., Tselfes N. (2008). *A simulated space-wise solution using GOCE kinematic orbits*. Bulletin of Geodesy and Geomatics. In print.
8. Braitenberg C., Pettenati F., Zadro M. (1997). *Spectral and classical methods in the evaluation of Moho undulations from gravity data: the NE-Italian Alps and isostasy*. Journal of Geodynamics, 23, 5-22.
9. Braitenberg C., Zadro M., Fang J., Wang Y., Hsu H.T. (2000). *Gravity inversion in Quinghai-Tibet plateau,* Physics and Chemistry of the Earth, 25/4, 381-386.
10. Braitenberg C., Wang Y., Fang J., Hsu H.T. (2003). *Spatial Variations of flexure parameters over the Tibet-Quinghai Plateau* Earth Planet. Sci. Lett., 205, 211-224.
11. Shin Y.H., Xu H., Braitenberg C., Fang J., Wang Y. (2007). *Moho undulations beneath Tibet from GRACE-integrated gravity data*, Geophys. J. Int., 1-15, DOI: 10.1111/j.1365-246X.2007.03457.x.
12. Allen P.A., Allen J.R. (2005). *Basin analysis: Principles and Applications*, 2nd edition. Blackwell Publishing, Oxford, 549p.
13. Braitenberg C., Ebbing J (2009). *The GRACE-satellite gravity and geoid fields in analysing large scale, cratonic or intracratonic basins*, Geophysical Prospecting, 57(4), 559-571.
14. Ebbing J., C. Braitenberg and S. Wienecke (2007) *Insights into the lithospheric structure and the tectonic setting of the Barents Sea region from isostatic considerations*, Geophys. J. Int., 171, 1390-1403, DOI: 10.1111/j.1365246X.2007.03602.x
15. Braitenberg C., Ebbing J (2009). *New insights into the basement structure of the west-Siberian basin from forward and inverse modelling of Grace satellite gravity data*,. J. Geophysical Res., 114, B06402, doi:10.1029/2008JB005799.
16. van Kann F., (2004) *Requirements and general principles of airborne gravity gradiometers for mineral exploration*, in R.J.L. Lane, editor, Airborne Gravity 2004 Abstracts from the ASEG-PESA Airborne Gravity 2004 Workshop: Geoscience Australia Record 2004/18, 1-5.
17. Parker R.L., (1972) *The rapid calculation of potential anomalies.* J. R. Astr. Soc. 31, 447–455.
18. Wieczorek M.A., Phillips J. (1998) *Potential anomalies on a sphere: applications to the thickness of the lunar crust,* J. Geophysical Res., 103, 1715-1724.